Elimination of Optical Self-Focusing by Population Trapping

Maneesh Jain, A. J. Merriam, A. Kasapi, G. Y. Yin, and S. E. Harris
Edward L. Ginzton Laboratory, Stanford University, Stanford, California 94305
(Received 10 July 1995)

We demonstrate a method for eliminating optical self-focusing and defocusing for a copropagating pair of intense laser beams whose frequencies differ by a Raman resonance. The lasers force the atoms of the medium into a population trapped state, thereby eliminating their contribution to the nonlinear refractive index.

PACS numbers: 42.50.Gy, 32.80.Lg, 42.50.Ne, 42.65.Jx

It is well known that intense laser beams, when tuned near to a resonance, will often break up into an unpredictable distribution of hot spots and filaments. This beam breakup and filament formation is initiated by self-focusing, which, in turn, is caused by the intensity-dependent refractive index [1].

In this Letter we show experimental results that demonstrate, at least for the near-ideal conditions described here, how optical self-focusing, defocusing, and filament formation may be eliminated. Our method is based on the use of two copropagating lasers to nearly instantaneously prepare an off-resonance population trapped state [2]. Once the atoms are in this state, then, irrespective of the relative intensity of the laser beams, there is no dipole moment and therefore no beam distortion at either laser wavelength. The essence of the theoretical problem is therefore to establish the necessary conditions and time scale for off-resonance trapped state preparation.

We apply two laser beams to a detuned three-state system (inset, Fig. 1). We assume that the common detuning, $\Delta\omega_3$, from state $|3\rangle$ is large as compared to both the strongest Rabi frequency and the linewidth of state $|3\rangle$, but still sufficiently small that the rotating wave approximation is valid. With these assumptions, the three-state Hamiltonian may be replaced by an effective two-state Hamiltonian [2,3]. With the envelopes of the fields denoted by $\Omega_p f(t)$ and $\Omega_c g(t)$, this two-state Hamiltonian is

$$H = -\frac{1}{4\Delta\omega_3}\begin{bmatrix} \Omega_p^2|f|^2 & \Omega_p\Omega_c f g^* \\ \Omega_p\Omega_c f^* g & \Omega_c^2|g|^2 \end{bmatrix} \equiv -\frac{1}{2}\begin{bmatrix} A|f|^2 & (AD)^{1/2} f g^* \\ (AD)^{1/2} f^* g & D|g|^2 \end{bmatrix}. \quad (1)$$

The diagonal elements of this Hamiltonian are the dynamic Stark shifts of states $|1\rangle$ and $|2\rangle$, which would result from the application of either laser, if alone. The off-diagonal elements are nonzero when both lasers are applied simultaneously. In general, the envelopes f and g are functions of both time and space.

One of the eigenvectors of this Hamiltonian has a zero eigenvalue and is termed a population trapped state. When all of the atoms are in the population trapped state, the two-by-two density matrix, in the bare basis, has the zeroth-order solution

$$\rho_{11}^{(0)} = \frac{D|g|^2}{A|f|^2 + D|g|^2}, \qquad \rho_{22}^{(0)} = \frac{A|f|^2}{A|f|^2 + D|g|^2},$$
$$\rho_{12}^{(0)} = -\frac{(AD)^{1/2} f g^*}{A|f|^2 + D|g|^2}. \quad (2)$$

To the extent that this solution can be established, there in no dipole moment and self-focusing, to all orders, is eliminated.

In describing the preparation of this state, one must distinguish between a medium of sufficiently low density that the electromagnetic fields which are applied at the cell input are unaffected by the medium, i.e., a refractively thin medium, and a high-density or refractively thick medium, where the fields are modified as they propagate. Defining β_p as the phase shift per unit length, relative to free space, of a propagating probe beam, if alone, i.e., $\beta_p = (2\pi/\lambda_p)(n - 1)$; a refractively thin or thick medium is characterized by $\beta_p L \ll 1$ or $\beta_p L \gg 1$, respectively.

For a propagating pulse pair in a realistic medium, the zeroth-order solution of Eq. (2) is never exact. If we write the density matrix elements as $\rho_{ij} = \rho_{ij}^{(0)} + \rho_{ij}^{(1)}$, then,

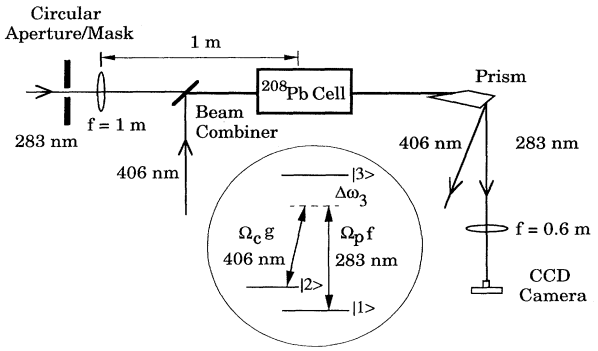

FIG. 1. Schematic of the experimental arrangement for studying the elimination of optical self-focusing and defocusing. States $|1\rangle$, $|2\rangle$, and $|3\rangle$ denote $6s^2 6p^2\,{}^3P_0$ (ground), $6s^2 6p^2\,{}^3P_2$ (metastable), and $6s^2 6p 7s\,{}^3P_1$ states of ^{208}Pb vapor.

without approximation [4],

$$\frac{\partial \rho_{12}^{(1)}}{\partial t} - j(AD)^{1/2} f g^* \rho_{22}^{(1)} - jq\rho_{12}^{(1)} = -\frac{\partial}{\partial t}\rho_{12}^{(0)} + j\Delta\tilde{\omega}\rho_{12}^{(0)},$$
$$\frac{\partial \rho_{22}^{(1)}}{\partial t} + \mathrm{Im}[(AD)^{1/2} f^* g \rho_{12}^{(1)}] = -\frac{\partial \rho_{22}^{(0)}}{\partial t}, \quad (3)$$

with the initial condition $\rho_{ij}^{(1)}(0) = \rho_{ij}(0) - \rho_{ij}^{(0)}(0)$. Here, $q = \frac{1}{2}(A|f|^2 - D|g|^2 + 2\Delta\tilde{\omega}_2)$ and $\Delta\tilde{\omega}_2 = \Delta\omega_2 + j\gamma_{21}$. γ_{21} is the dephasing rate of the $|1\rangle$-$|2\rangle$ transition and $\Delta\omega_2 = (\omega_2 - \omega_1) - (\omega_p - \omega_c)$. The zeroth-order solution is corrected by both the time variation of the applied fields (which leads to the group velocity delay) and by dephasing and detuning from the $|1\rangle$-$|2\rangle$ transition.

With $\nabla_t^2 \equiv \partial^2/\partial x^2 + \partial^2/\partial y^2$ the coupled envelope equations that describe the propagating pulse pair in the paraxial approximation are

$$\left(\frac{\partial}{\partial z} + \frac{j}{2k_p}\nabla_t^2 + \frac{1}{c}\frac{\partial}{\partial t}\right) f = -j\beta_p\left[\tilde{\rho}_{11}^{(1)} + \sqrt{\frac{D}{A}}\frac{g}{f}\tilde{\rho}_{12}^{(1)}\right] f,$$
$$\left(\frac{\partial}{\partial z} + \frac{j}{2k_c}\nabla_t^2 + \frac{1}{c}\frac{\partial}{\partial t}\right) g = -j\beta_c\left[\tilde{\rho}_{22}^{(1)} + \sqrt{\frac{A}{D}}\frac{f}{g}\tilde{\rho}_{12}^{(1)*}\right] g. \quad (4)$$

The tildes on $\rho_{12}^{(1)}$ and $\rho_{22}^{(1)}$ allow for averaging over the inhomogeneous linewidth, $\delta\omega_D$, of the $|1\rangle$-$|2\rangle$ transition. The quantities $\beta_p = \omega_p N|\mu_{13}|^2/2\epsilon_0 c\hbar\Delta\omega_3$, $\beta_c = \omega_c N|\mu_{23}|^2/2\epsilon_0 c\hbar\Delta\omega_3$, and, in free space, $k_p = 2\pi/\lambda_p$, $k_c = 2\pi/\lambda_c$. If $\tilde{\rho}_{ij}^{(1)} = 0$, the beams propagate as they would in free space.

To initiate the population trapped state in an optically thin medium with all of the atoms in the ground state, the coupling laser field $\Omega_c g$ is applied with the probe field $\Omega_p f$ still equal to zero. This causes the population trapped eigenvector at $t = 0$ to coincide with the ground state of the atom [Eq. (2)], so that $\rho_{ij}^{(1)}(0) = 0$. The probe field is then increased sufficiently slowly, with the coupling field sufficiently strong [Eq. (3)], so that at all times $|\tilde{\rho}_{12}^{(1)}| \ll 1$. This method of initiation is similar to that used by Grischkowsky for two-state systems [1], and by Hioe [5] and Kuklinski *et al.* [6] for three-state systems. For these conditions, in an optically thin medium, the time scale for establishing the population trapped state is the inverse of the dynamic Stark shift parameter D.

In a refractively thick medium, $\beta_p L \gg 1$, the condition $|\tilde{\rho}_{12}^{(1)}| \ll 1$ is no longer sufficient and, instead, the right-hand side of Eq. (4) must be made sufficiently small. We also require that the coupling pulse be present for the time that it takes for the probe pulse to propagate through the medium. Numerical work [4], which allows for z propagation but not for transverse variation and also neglects inhomogeneous broadening, shows that self-consistent preparation in a refractively thick medium is possible and is similar to on-resonant preparation [7]. Here, the essential time scale for state preparation is the group delay time of the propagating probe pulse [4].

Before describing our experiment, we cite some earlier work. In the context of atomic coherence and interference effects, Scully [8], Agarwal [9], and Rathe *et al.* [10] note possibilities for modifying the near-resonance refractive index. Kocharovskaya and Mandel [11] describe the propagation of monochromatic fields in population trapped media. Light shifts in three-state systems are discussed by Weitz, Young, and Chu [12]. Xiao *et al.* [13] experimentally study near-resonance dispersion. Moseley *et al.* [14] describe the use of a strong coupling field to focus a weak probe. Kasapi *et al.* [15] demonstrate slow group velocities and high quality beam propagation through otherwise strongly absorbing Pb vapor.

A schematic of our experiment is shown in Fig. 1. The laser system is the same as that of Kasapi *et al.* [15]. The 406-nm coupling laser and the 283-nm probe laser beams are obtained from frequency-doubled and frequency-tripled Ti:sapphire laser systems. Each system is seeded by an external-cavity diode laser and operates in a single longitudinal mode with a long-term frequency stability of under 100 MHz. In this work the pulse lengths of the coupling and probe laser pulses are 120 and 14 ns, and the pulse energies are typically 500 and 10 μJ, respectively, which correspond to typical power densities of 1 to 10 MW/cm^2.

We work with 99.97% isotopically pure lead vapor (^{208}Pb) and, in order to create an ideal three-state system, the probe and coupling laser beams have opposite circular polarization. A 10-cm-long sealed fused-silica side arm cell is used at a typical atom density of about 4×10^{15} atoms/cm^3. This density is determined by measuring the full width at the $1/e$ points (2.7 cm^{-1}) of the (optically thick) transmission profile and also the Lorentzian portion of the $|1\rangle$-$|3\rangle$ transition linewidth (0.0016 cm^{-1}), and then combining these values with the cell length, probe transition Doppler width (0.06 cm^{-1}), and oscillator strength ($gf = 0.197$). In much of this work, the probe and coupling lasers are detuned from resonance by ± 20 cm^{-1}, which, at typical cell densities, is 12 500 Lorentzian linewidths.

We first describe the geometry and experimental results for eliminating self-focusing (Fig. 1). A collimated probe beam is incident on a 3.2-mm circular aperture. A 1-m lens focuses the beam so that, at the cell center, the probe beam diameter ($1/e$) and the first zero of the Airy pattern are 0.11 and 0.22 mm, respectively. A second lens ($f = 0.63$ m) is positioned to image the 3.2-mm aperture onto a charge coupled device (CCD) camera. The coupling laser at 406 nm is focused so that its diameter at the cell center is 0.4 mm. For self-focusing, the probe is tuned 20 cm^{-1} to the blue side of the 283-nm transition. At the measured atom density of $4 \times 10^{15} \pm 20\%$ atoms/cm^3, $\beta_p L = 56$.

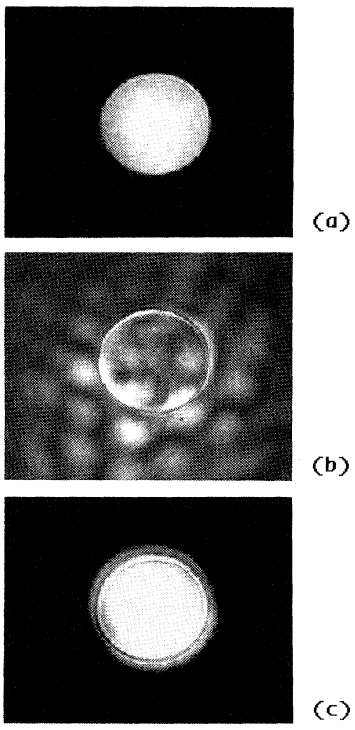

FIG. 2. Elimination of optical self-focusing. This figure shows the CCD camera images of the 3.2-mm apertured probe. For this figure, $\beta_0 L = 56$. (a) Weak probe alone, $A = 6 \times 10^{-5}\,\mathrm{cm}^{-1}$; (b) strong probe alone, $A = 0.34\,\mathrm{cm}^{-1}$; (c) strong probe and coupling laser, $A = 0.34\,\mathrm{cm}^{-1}$, $D = 0.12\,\mathrm{cm}^{-1}$. The beam filamentation of part (b) is eliminated by applying the coupling laser in part (c).

Figure 2 shows the results of this experiment. Figure 2(a) shows the CCD camera image of the 3.2-mm aperture when the weak probe (alone) is transmitted through the cell. Here, the Stark shift parameter of state $|1\rangle$ is $A = 6 \times 10^{-5}\,\mathrm{cm}^{-1}$, and there is no observable image distortion. In Fig. 2(b) the power density of the probe is increased by about a factor of 10^4 ($A = 0.34\,\mathrm{cm}^{-1}$), and severe distortion and filament formation of the imaged aperture is observed. In Fig. 2(c) the coupling laser is turned on ($D = 0.12\,\mathrm{cm}^{-1}$, $D/\delta\omega_D \sim 7$) and tuned to two-photon resonance. The probe intensity is the same as in Fig. 2(b). We observe that the image is now restored to nearly the quality of the image in Fig. 2(a).

In the next experiment we study the suppression of optical self-defocusing. For this experiment, the probe and coupling lasers are tuned $20\,\mathrm{cm}^{-1}$ to the red side of the resonance transition. We replace the CCD camera (Fig. 1) with a photodiode and place a 3-mm-diam beam block in front of it, so that the image of the circular aperture is completely blocked under cold-cell or weak-probe conditions. As the probe intensity is increased, defocusing occurs, and we obtain a 283-nm signal from this detector. This signal is averaged over 200 shots and normalized to its value with the coupling laser turned off.

Figure 3(a) shows the dependence of the 283-nm signal on the coupling laser intensity. In this experiment, $\beta_p L = 42$. At $D/D_{\mathrm{Doppler}} = 9$, the defocused signal is reduced by a factor of 40. Even with D/D_{Doppler} less than unity, a significant reduction of the signal is observed.

In Fig. 3(b) we study the relative 283-nm intensity as a function of very small changes of the probe frequency and therefore of the detuning $\Delta\omega_2$ from two-photon resonance. We note that detunings much smaller than the two-photon Doppler width negate the suppression of self-defocusing.

In the experiments just described, $|\Delta\omega_3|$ was $20\,\mathrm{cm}^{-1}$ and the nonlinear refractive index was dominated by the first term in its series expansion. In order to ascertain whether higher order nonlinearities could also be removed, the detuning was reduced to $0.45\,\mathrm{cm}^{-1}$. For $\Omega_p = 0.9\,\mathrm{cm}^{-1}$, the ratio $\Omega_p/\Delta\omega_3 = 2$ and a series expansion is no longer applicable. We examined self-

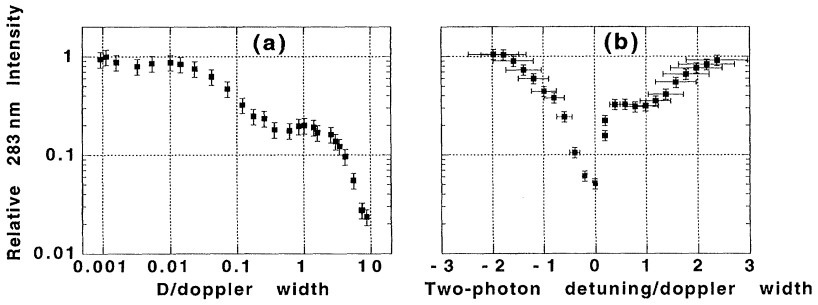

FIG. 3. Suppression of optical self-defocusing. A 3-mm beam block is placed between the 2-mm image of the aperture and the photodiode. When the probe is strong, it is defocused and much of the light passes the beam block. We measure this light as a function of (a) the parameter D normalized to the Doppler width, $\delta\omega_D = 0.018\,\mathrm{cm}^{-1}$ (other parameters are $A = 0.072\,\mathrm{cm}^{-1}$, $N = 3.0 \times 10^{15} \pm 20\%$ atoms/cm^3, $\gamma_{21} = 3 \times 10^{-4}\,\mathrm{cm}^{-1}$) and (b) as a function of the detuning from two-photon resonance (here, $A = 0.55\,\mathrm{cm}^{-1}$, $D = 0.090\,\mathrm{cm}^{-1}$, $N = 3.5 \times 10^{15} \pm 20\%$ atoms/cm^3). The error bars denote the spread of the data.

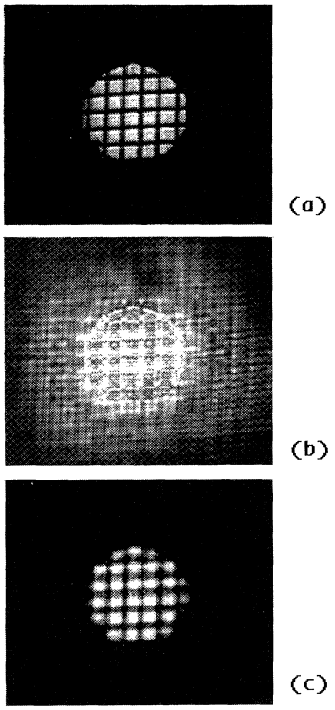

FIG. 4. Elimination of higher-order nonlinears. In this experiment the common detuning $\Delta\omega_3$ is reduced from 20 to 0.45 cm^{-1}. (a) Weak probe alone, $\Omega_p = 0.02$ cm^{-1}; (b) strong probe alone, $\Omega_p = 0.9$ cm^{-1}; (c) probe and coupling laser, $\Omega_p = 0.9$ cm^{-1}, $\Omega_c = 0.8$ cm^{-1}.

focusing in this regime by replacing the circular aperture with a 52-line/in., 0.1-mm-thick wire, amplitude mask. At the cell center, the higher spatial frequencies of the amplitude mask map into positions that are further off axis. The diameter of the coupling laser beam (at the cell center) was therefore increased to 0.9 mm. Also, to allow for a weak-probe transmission of greater than 95%, the atom density was reduced to 3×10^{13} atoms/cm^3 ($\beta_p L = 19$).

The results of this experiment are shown in Fig. 4. Figure 4(a) shows the CCD camera image of the weak probe, $\Omega_p = 0.02\,cm^{-1}$, alone. Figure 4(b) shows the CCD image with the probe intensity increased so that $\Omega_p = 0.9\,cm^{-1}$ and with Ω_c still equal to zero. Substantial distortion is observed. Figure 4(c) shows the image with a peak (beam center) coupling laser Rabi frequency of $\Omega_c = 0.8$ cm^{-1}. To the eye, the corrected image is now of almost the same quality as that of the weak probe alone.

The results presented here demonstrate a technique for the elimination of optical self-focusing and defocusing. They also provide strong evidence for the preparation of an off-resonance population trapped state. As further evidence for this preparation we note that at a detuning of 20 cm^{-1} and under experimental conditions with $\beta_p L = 56$ we observe a weak-probe pulse delay of 6 ns. This corresponds to a relative group velocity of $c/Vg = 18$, which is in agreement with theory. (At this detuning and density, a probe, if alone, has a calculated delay and relative group velocity of 0.015 ns and $c/Vg = 1.05$.)

In summary, we have shown how copropagating laser beams may be used to prepare an off-resonance population trapped state in a refractively thick medium, and how this state may be used to suppress optical self-focusing and defocusing. We mention that the rotating wave approximation is critical for the preparation of a perfect population trapped state, and that the possibility of extending these results to detunings greater than a few thousand wave numbers and to multistate systems will require further study.

The authors thank Hui Xia for his assistance with the experiment. This research was supported by the U.S. Army Research Office, the U.S. Air Force Office of Scientific Research, and the U.S. Office of Naval Research.

[1] D. Grischkowsky, Phys. Rev. Lett. **24**, 866 (1970); D. Grischkowsky and J. A. Armstrong, Phys. Rev. A **6**, 1566 (1972).
[2] S. E. Harris, Opt. Lett. **19**, 2018 (1994).
[3] A. H. Toor and M. S. Zubairy, Phys. Rev. A **45**, 4951 (1992).
[4] S. E. Harris (unpublished).
[5] F. T. Hioe, Phys. Lett. **99A**, 150 (1983).
[6] J. R. Kuklinski, U. Gaubatz, F. T. Hioe, and K. Bergmann, Phys. Rev. A **40**, 6741 (1989).
[7] J. H. Eberly, M. L. Pons, and H. R. Haq, Phys. Rev. Lett. **72**, 56 (1994); R. Grobe, F. T. Hio, and J. H. Eberly, Phys. Rev. Lett. **73**, 3183 (1994); S. E. Harris, Phys. Rev. Lett. **72**, 52 (1994); S. E. Harris and Zhen-Fei Luo, Phys. Rev. A **52**, R928 (1995).
[8] M. O. Scully, Phys. Rev. Lett. **67**, 1855 (1991).
[9] G. S. Agarwal, Phys. Rev. Lett. **71**, 1351 (1993).
[10] U. Rathe, M. Fleischhauer, Shi-Yao Zhu, T. W. Hänsch, and M. O. Scully, Phys. Rev. A **47**, 4994 (1993).
[11] O. Kocharovskaya and P. Mandel, Phys. Rev. A **42**, 523 (1990).
[12] M. Weitz, B. C. Young, and S. Chu, Phys. Rev. A **50**, 2438 (1994).
[13] M. Xiao, Y.-Q. Li, S.-Z. Jin, and J. Gea-Banacloche, Phys. Rev. Lett. **74**, 666 (1995).
[14] R. R. Moseley, S. Shepherd, D. J. Fulton, B. D. Sinclair, and M. H. Dunn, Phys. Rev. Lett. **74**, 670 (1995).
[15] A. Kasapi, M. Jain, G. Y. Yin, and S. E. Harris, Phys. Rev. Lett. **74**, 2447 (1995); A. Kasapi, G. Y. Yin, and M. Jain, "A Pulsed Ti:Sapphire Laser Seeded Off the Gain Peak" (to be published).

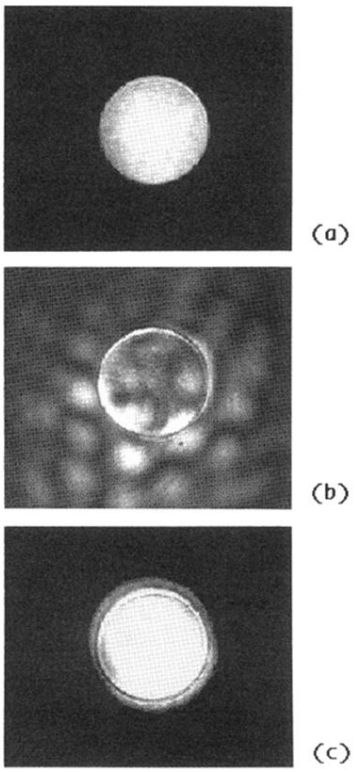

FIG. 2. Elimination of optical self-focusing. This figure shows the CCD camera images of the 3.2-mm apertured probe. For this figure, $\beta_0 L = 56$. (a) Weak probe alone, $A = 6 \times 10^{-5}\,\mathrm{cm}^{-1}$; (b) strong probe alone, $A = 0.34\ \mathrm{cm}^{-1}$; (c) strong probe and coupling laser, $A = 0.34\ \mathrm{cm}^{-1}$, $D = 0.12\ \mathrm{cm}^{-1}$. The beam filamentation of part (b) is eliminated by applying the coupling laser in part (c).

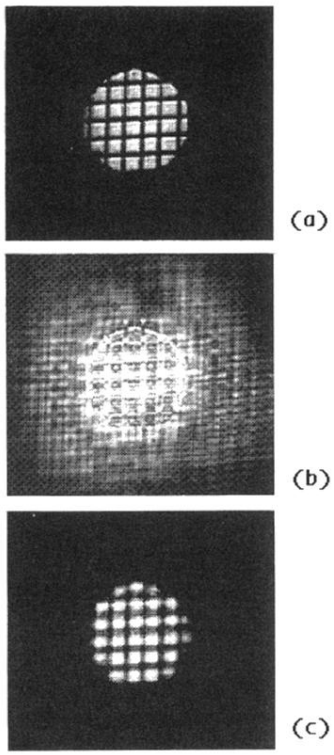

FIG. 4. Elimination of higher-order nonlinears. In this experiment the common detuning $\Delta\omega_3$ is reduced from 20 to 0.45 cm^{-1}. (a) Weak probe alone, $\Omega_p = 0.02$ cm^{-1}; (b) strong probe alone, $\Omega_p = 0.9$ cm^{-1}; (c) probe and coupling laser, $\Omega_p = 0.9$ cm^{-1}, $\Omega_c = 0.8$ cm^{-1}.